

EFFICIENT CIS-LUNAR TRAJECTORIES

Author: Kevin E. Post

Boeing Defense Space & Security, Houston, TX, United States, kevin.e.post@boeing.com

Edward Belbruno

Innovative Orbital Design, Inc & Princeton University, Princeton, NJ, United States, belbruno@Princeton.edu

Francesco Topputo

Aerospace Engineering Department, Politecnico di Milano, Milan, Italy, topputo@aero.polimi.it

Twenty years ago, the theoretical notions of low-energy transfers were put to test with the Japanese spacecraft, *Hiten*. With the successful implementation of the low-energy transfer trajectory discovered by Belbruno, *Hiten* exposed the available option space for mission designers seeking efficient transfers and planetary captures.

Integrated mission designs utilizing these kinds of low-energy transfers would enhance the operational flexibility of an Exploration Platform operating within the Earth-Moon Lagrange Point 2 (EML2) vicinity. This paper provides a brief rationale for the use of low-energy transfers in human space exploration architectures, considering how flexible path architectures, by definition, require finding an architectural ‘sweet spot’ in the convergence of efficiency, resilience, and cost. It then examines the types of high and low energy transfers that could be performed during the operation of such a facility, taking advantage of the natural dynamics of the Earth-Moon system in such a way as to maximize mass delivery while minimizing the propellant used in the transfer.

We conclude that in moving human exploration beyond Low Earth Orbit (LEO), the integration of high and low energy transfers in an EML2 exploration platform mission design architecture provides the flexibility to perform meaningful, near-term missions which will inform space-faring nations of the consequences and risks involved in deep-space exploration. Additionally, the surface-destination based missions are allowed to continue to be explored with regard to necessary technology and investment decisions, without having to make the specific investment commitments in the near-term for surface-based missions.

I. INTRODUCTION

Historically, the Hohmann transfer has been the foundation of space travel and mission design. Walter Hohmann published a book in 1925 where he demonstrated this orbital transfer. The primary utilization of the Hohmann transfer is for designing orbital transfers defined by the two-body problem. Belbruno addresses some of the limitations that arise from applying the two-body Hohmann transfer to interplanetary transfers that involve four-body problem definition, such as the Earth to Moon transfer. He concludes by saying that although breaking down the four-body problem into a series of two-body problems is not dynamically correct, it suffices as a methodology for the mission designer since the transfers have a high energy associated with them.¹ A spacecraft, in order to use these transfers, has to induce a relatively high delta-velocity via its propulsion system in order to perform such transfers, requiring significant amounts of propellant.

Rather than breaking down an interplanetary transfer into patched-conic trajectories of Hohmann transfer origin, what if the mission designer chose to put another tool in their mission design toolbox?, a tool that

integrates the natural dynamical systems defined by the events and processes of planetary movement. Definition of these astronomical dynamic systems has been evolving for some time; however, the application of these systems to the intentional movement of spacecraft is relatively new. In 1986, E. Belbruno theorized a Weak Stability Boundary as an element of planetary dynamical systems that could be utilized to create transfers between planetary bodies which take advantage of the natural dynamical system created by their movement to transfer a spacecraft from one location to another with very little delta-velocity (ΔV) induced by the spacecraft. Four years later, about twenty years ago, these theoretical notions of low-energy transfers were put to test with the Japanese spacecraft, *Hiten*. With the successful implementation of the low-energy transfer trajectory discovered by Belbruno, *Hiten* exposed the available option space for mission designers seeking efficient transfers and planetary captures.

This paper explores the use of this kind of transfer in support of a human-tended Exploration Platform located at the Earth-Moon libration point 2 (EML2), a central strategy in defining a global space architecture which

balances efficiency and resilience. It provides an overview of dynamical systems and a discussion of specific analysis results that investigate these low-energy transfers to EML2.

II. DEFINING TRAJECTORY & PROPULSION STRATEGIES

A concept for an EML2 facility has been proposed by Raftery and Hoffman²; this facility is an international endeavor based upon the agreements already in place for the International Space Station (ISS). An International Core Module and a Docking Node provide for an early deployment, activation, and use of this human-tended facility. Each element provides specific functionality that is required for the initial missions. Additionally, the early configuration supports initial performance estimates for the Space Launch System (SLS). With increased mission duration and celestial body destinations defined, the Exploration Platform increases its functionality to support these other missions. Figure 1 provides an overview of the element composition of the facility with associated functions and mission support.

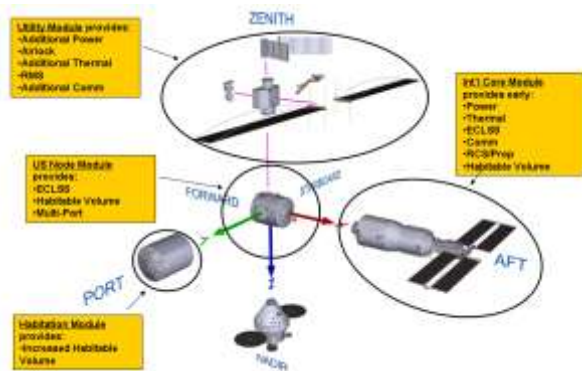


Figure 1 Exploration Platform

Integrated mission designs utilizing both high-energy and low-energy transfers would enhance the operational flexibility of an International Exploration Platform operating within the EML2 vicinity. When considering the use of both types of transfers in space architectures, the spacecraft propulsion system design needs to incorporate the anticipated mission requirements. In general, the high-energy transfer would require a high-thrust propulsion system while a low-energy transfer would take advantage of the low-thrust propulsion option.

High-Energy Transfers

A boat traveling across or against tidal flows requires a lot of energy to overcome the effects of the tide that can push against the direction the boat intends to travel. Additionally, the velocity of travel becomes

important in not only overcoming the tidal force but also in terms of the time of travel. Similarly, travel through space encounters similar type of forces which require a high level of energy to overcome in order for the spacecraft to travel to its intended destination. Overcoming and utilizing the gravitational forces between celestial bodies can tax the spacecraft and mission designer attempting to create a cost-effective transportation system.

Generally speaking, the Hohmann transfer is associated with high-energy as a spacecraft works through the gravitational field of different celestial bodies⁴. Departing one planet for another, also known as ‘injection’, requires a significant amount of energy to leave the gravity well of the originating planet. Also, during lengthy high-energy transfers, the spacecraft would need to perform corrections while traveling in the gravity well in addition to maneuvers used to transition from between gravity wells. When arriving at its destination, the spacecraft traveling on a high-energy transfer then needs to perform a ‘capture’ maneuver where any excess energy is removed from the transfer, allowing the spacecraft to settle into an orbit about the destination.

High-Thrust Propulsion

All of this energy expended in the travel against the gravitational ‘tide’ requires a source. In the case of a boat traveling across the water, often times the most reliable source is a powerful engine that is capable of overcoming the natural forces of the tide. With spacecraft it is very similar; a propulsion system providing high-thrust capability is designed into the spacecraft. In these systems, the thrust level selected is guided by the structural loads, trip duration, overall mass of the spacecraft, including the propellant required for its intended use, the trajectories or transfers selected in the mission design, and the gravitational forces expected.

Consequently, large (relative to spacecraft size), high-thrust propulsion systems are typically required when using high-energy transfers in the mission design. These transfers require elevated delta-velocity (ΔV) which translates into more propellant for a given specific impulse.

If there are other transfer options available to be explored wherein the overall architecture can benefit, then these should be explored in the context of optimizing the mission design space within the constraints of stakeholder requirements. The low-energy transfer offers such an option.

Low-Energy Transfers

Many types of marine operators utilize the natural forces of the tides to take advantage of the energy savings of such a transit. Across the Earth’s oceans,

there are currents that are utilized by shipping companies to reduce the amount of energy expended by the vessel. These currents are natural phenomena of the sea. In the context of space travel, there also exists a type of natural ‘current’ that allow a spacecraft to use less energy to move between locations. The nature of these natural systems is discussed further in section III of this paper, but they are introduced here to facilitate the discussion between energy transfers and propulsion systems.

Low-energy transfers take advantage of the natural dynamics between and around celestial bodies. These dynamics are highly sensitive ‘phase-space’ areas that not only can take advantage of an efficient, low-thrust, propulsion system, but could be said to require the use of low-thrust propulsion so as to not unduly perturb the spacecraft outside of the natural dynamic ‘phase-space’ and lose efficiency in the process. Like a marine vessel traveling with the current, the spacecraft on a low-energy transfer needs to only induce small amounts of delta-velocity to not only get into the current, but also to travel along it to its destination where it could arrive at what is essentially a ballistic capture.

Low-Thrust Propulsion

The spacecraft and mission designer take advantage of low-energy trajectories by designing in a low-thrust propulsion system. These systems have a high specific impulse and use thrust to power ratios in the range of 0.025–0.059. Current low-thrust propulsion systems that have flight experience are smaller solar-electric propulsion (SEP) systems. They use the power generated by the solar arrays to ionize an inert gas before accelerating the charged particles at very high exit velocities.

In concept design, the Exploration Platform integrates both high-thrust and low-thrust propulsion systems to take advantage of the low-energy transfer ‘phase-space’ that is in the Lunar vicinity. The conceptual mission design for an Exploration Platform at EML2 seeks to take advantage of both the high-energy transfer and low-energy transfer option space to create a global exploration architecture that balances efficiency and resilience within a cost-constrained environment.

III. DYNAMICAL SYSTEMS THEORY IN TRAJECTORY DESIGN

The use of the Hohmann transfer enables a spacecraft to go from the Earth to the Moon within a short time of flight on the order of a few days, however, upon lunar arrival it is moving fairly fast with respect to the Moon, with a relative velocity on the order of 1 km/s. A substantial ΔV is required to slow down to become captured into a low lunar orbit. This can require

a significant amount of propellant and hence can be expensive. Is there a better way to go into lunar orbit?

This motivated the development of transfers from the Earth to the Moon by E. Belbuno in 1986¹¹ that had the property that a spacecraft would be captured automatically into lunar orbit, with no maneuvers required – this is called *ballistic capture*¹. This was accomplished by using methods of dynamical systems theory:

First- a region is estimated about the Moon where ballistic capture can occur, called a weak stability boundary (WSB). This region exists in position-velocity space. It exists due to the interaction of the Earth and Moon gravitational fields. A spacecraft is in this region, at given distance from the Moon, and moving in a given direction, if it has a critical velocity.

Second - a trajectory is determined which goes from the Earth to the WSB, at the desired lunar altitude moving in a desired direction with respect to the Moon, and with the required velocity. The trajectory follows a natural pathway, or channel, called a *manifold*, that exists in position-velocity space^{1,5}. These channels exist due to the interaction of the Earth-Moon gravitational fields. This methodology, called WSB Theory, which determines ballistic capture transfers (also called WSB transfers), was dramatically validated in 1992 with the rescue of a Japanese lunar mission, by getting its spacecraft, *Hiten*, to the Moon on October 2, 1992^{1,6,7,8}. The route that *Hiten* took from the Earth first goes out far beyond the Moon to about four times the Earth-Moon distance, then falls back to the Moon along a manifold, where it arrives with the correct velocity to be in the WSB at the desired altitude and hence is ballistically captured. This route took about four months and is called an *exterior WSB transfer*. It is an example of a *low energy transfer*. It is low energy since it requires negligible ΔV for lunar capture, as well as capture about L_1 , L_2 points, and also because it utilizes natural manifold pathways. The term ‘exterior’ is used since the transfer goes far beyond the orbit of the Moon. There are also WSB transfers that remain essentially within the Moon’s orbit, and they are called *interior WSB transfers*, discussed below. It is remarked that these transfers are sometimes generally referred to as ‘ballistic capture transfers’, ‘low energy transfers’, although these terms are less specific.

The dynamics of motion of a spacecraft within the WSB region is sensitive, and tiny ΔV ’s can be used to effect large changes of the motion or stabilize the motion for tiny ΔV . In this sense the motion is unstable and even chaotic since the pathway structure is very complicated and can lead to infinitely many possible trajectories with radically different directions with a tiny ΔV application. However, this is ideal for efficient trajectory design using little propellant.

The exterior WSB transfer generally passes near the location of exterior Earth-Moon Lagrange point L_2 on the anti-Earth-Moon line of the Moon, although it doesn't have pass too closely. It can also pass near Earth-Sun L_1 point, although this is not necessary. To find this transfer, one has to model the gravity of not just the Earth and Moon, but also the Sun, making a four-body problem between the Earth, Moon, Sun and spacecraft. The spacecraft moves out about 1.5 million kilometers from the Earth, at the approximate distance of the Earth-Sun collinear Lagrange points L_1 , L_2 . Another mission to use this transfer was NASA's GRAIL spacecraft in 2011, providing a second use of the exterior WSB transfer. A detailed mathematical description of the exterior and interior WSB transfers can be found in Reference 1.

The first WSB transfer that was found in 1986 was an interior WSB transfer. It only requires the modeling of a three-body problem between the Earth, Moon, and spacecraft. That transfer was designed for a spacecraft using solar electric propulsion, called LGAS (Lunar Get Away Special) taking about 1.5 years to spiral away from the Earth using the electric engines, then transfer from the Earth to the Moon on a WSB transfer. Its design was eventually used by ESA's SMART-1 spacecraft in 2004^{8,12}. This transfer generally passes near to the interior Lagrange point L_1 . It follows the manifold pathways between the Earth and Moon, leading to the lunar WSB and hence to ballistic capture^{1,8,12}. As we will discuss in this paper, the interior transfer can be designed to go to ballistic capture about L_2 as well. The interior transfer has the property that the manifolds the trajectory uses, don't get any closer to the Earth than about 60,000 km, whereas the exterior transfer can start at any altitude from the Earth.¹

The first description of such transfers using dynamical systems and manifolds was accomplished in 1994¹⁰. This description was done several years later in more detail in 2001 by G. Marsden et al.¹³ Although the WSB is computed numerically using a well defined algorithm, its mathematical and geometric nature has been elusive due to its complexity. A significant insight into its nature was accomplished by F. Garcia and G. Gomez in 2007, showing an exquisite geometric structure that is fractal in nature, in multi-dimensions¹⁴. The manifold structure of this region was partially uncovered by E. Belbruno, M. Gidea and F. Topputo in 2011¹⁵. The main result is that the lissajous (Lyapunov) orbits about the Earth-Moon L_1 and L_2 points together with the manifold pathways that lead to them, which intersect in an infinitely complex manner about the Moon, forming a fractal region, is equivalent to the WSB. Thus, the WSB consists of all the manifold pathways associated not just about the Moon, but with the L_1 , L_2 points. These results are also true for the Earth-Sun Lagrange points L_1 , L_2 and WSB about the

Earth due to the Earth-Sun gravitational interaction. Thus, the WSB is equivalent to all the manifold pathways in the Earth-Moon system, as well as the Earth-Moon-Sun system, that ultimately approach the Lyapunov orbits about L_1 and L_2 , in either system in forwards time. These manifolds in backwards time, wrap around the Moon, or Earth, in position-velocity space, forming a highly complex region. This framework is also applicable to the Jupiter system, Saturn system, etc.

An exciting development is the design of low energy trajectories for spacecraft using a hybrid propulsion system with both chemical and electric thrusters. This design incorporates new optimization methods that can be applied to the sensitive low energy trajectories using electric propulsion while moving in the WSB about the Moon, to and from the L_1 and L_2 regions, and also utilizing the manifold pathways. By optimizing on low energy trajectories, transfers can be obtained from the Earth into orbit about the L_1 and L_2 points, or about the Moon, that use substantially less propellant than the Hohmann transfer.

We present results below that determine new low energy pathways from the Earth into orbit about the Earth-Moon L_2 point using a newly developed optimization method¹⁷. Hybrid propulsion systems using both chemical and electric propulsion are used as well as purely chemical propulsion. The trajectories are shown to be substantially more efficient than the Hohmann transfer, which for one system we consider, doesn't even have sufficient propellant to go into orbit about L_2 , whereas the new route accomplishes orbit about L_2 with significant margin. The pathways we consider first are based on interior WSB trajectories and the second case we consider utilize the exterior WSB transfer.

Overview of Dynamical Systems Methodology, The Three-Body Problem, Manifolds, and the Weak Stability Boundary

The subject of dynamical systems has existed since the time of H. Poincare', who laid the foundations for the field in the latter 19th century. His inspiration for developing this subject came from celestial mechanics, and in particular the three-body problem for the motion of three mass particles, or bodies, under their mutual gravitational interactions. He published a celebrated three volume set of books⁹. Since then the field has evolved significantly.

Dynamical systems concerns itself with obtaining a geometrical understanding the behavior of solutions of ordinary differential equations that are used to define a dynamical process. Prior to the work of Poincare, people tried to find explicit solutions to the three-body problem for each of the three bodies, for their positions

as a function of time using infinite series expansions. It was found that these expansions were not well defined since they did not converge. Poincare's approach was not to try and find explicit closed form solutions for the motions of the three bodies, but rather look for special solutions, not in explicit form, but rather as geometric objects.

For example, a periodic orbit is a trajectory of a particle that keeps returning to its initial position in the same time interval. An example of this would be a circular orbit of period T years of an asteroid about the Sun, in the idealized case where a pure circular orbit could exist. We let Jupiter be the third body. If we let t represent time, and $x(t) = (x_1(t), x_2(t), x_3(t))$ be the position of the asteroid about the Sun as a function of time, where the Sun is at the origin of a coordinate system (x,y,z) , then $x(t+T) = x(t)$. Since the orbit keeps returning to its same location every T years, then Poincare reasoned that it is not necessary to know the entire orbit, but only its location at one point. He did this by taking a plane P and placing it so it was transversal to the orbit, so the orbit intersected, or cut, P in one point, p of the periodic orbit. This one point p on P then represents the entire orbit. He then considered another general solution of the differential equations for the motion of a particle near the orbit of the asteroid. He took its initial position x_0 on P near p . When it cycled around the Sun and returned to P after a time near T , it need not return to its starting point x_0 since it need not be periodic. Rather, it would intersect P at another point near x_0 , say y^* . In this sense, the point x_0 is mapped into the point y by a mapping, M , defined by the motion of the trajectory. So, we have that $y^* = M(x_0)$. As the trajectory goes around the Sun again and returns to P , we obtain another point $y^{**} = M(y^*)$, etc. As the trajectory keeps cycling around the Sun over and over, it keeps intersecting P in other points. In this way, all these points represent the motion of the particle. The motion near the asteroid can therefore be viewed on P as a set of points generated by the mapping function M . This plane P is called a Poincare section. The resultant set of points on P after the trajectory goes around infinitely many times represents the dynamics of the particle defined by M . Understanding the properties of M then yields information on the properties of the dynamics. The periodic orbit is represented as a fixed point of M since $Mp = p$.

This reduction to a mapping function represented a new approach to understanding solutions to differential equations, and in this case the three-body problem.

A general approach taken by dynamical systems is to study geometric objects in the position-velocity space where the motion of a particle is constrained. At this point, we define the system of differential equations we will need in our analysis to discuss this in further detail.

We consider the motion of a spacecraft, SC, in the Earth-Moon system. The particles we consider are the three bodies – $P_1 = \text{Earth (E)}$, $P_2 = \text{Moon (M)}$, $P_3 = \text{SC}$. The problem is idealized so that we make the following assumptions: (1) The mass of SC is assumed to be negligible, and hence 0, with respect to the mass m_1 of E and the mass m_2 of M, (2) The motion of M about E is assumed to be a perfect circle of constant circular velocity, (3) The motion of SC is constrained to the plane of motion of E and M. This is called the planar circular restricted three-body problem for the motion of SC in the gravitational field generated by E,M.¹ It is this problem that inspired Poincare. Although it seems fairly simple with all the assumptions, the motion of SC can be extremely complex and chaotic in nature. In fact, to this day, the general motion of SC is not completely understood, especially when SC moves about M. We can write the differential equations for the motion of SC in a rotating coordinate system (x,y) . This is a coordinate system that rotates uniformly, with frequency w , with the circular motion of M about E. The system of differential equations for the motion of SC is given by,

$$\begin{aligned} d^2x/dt^2 - 2 dy/dt &= F_x \\ d^2y/dt^2 + 2 dx/dt &= F_y, \end{aligned}$$

where F_x is the partial derivative of F wrt x , and

$$F(x,y) = (1/2)(x^2 + y^2) + (1-m)/r_1 + m/r_2 + (1/2)m(1-m),$$

$$r_1^2 = (x + m)^2 + y^2, \quad r_2^2 = (x - (1-m))^2 + y^2$$

We have put E and M on the x -axis where they are fixed. E is at $(-m,0)$ and M is at $(1-m,0)$ $m = m_2/(m_1+m_2) = .012...$ The units are scaled so that the distance from E to M is 1 and $w=1$. The center of mass of E, M is at the origin, (See Figure 2)

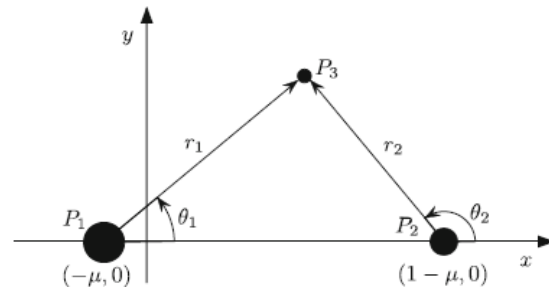


Figure 2 Rotating reference frame ($m = \mu$)

The Jacobi energy $J(x,y,dx/dt,dy/dt)$ is a constant(integral) of the motion – so that along a

solution of the differential equations, $Q(t) = (x(t), y(t), (dx/dt)(t), (dy/dt)(t))$, we have that $J(Q(t)) = C = \text{constant}$.

C is called the Jacobi constant, and where

$$J = 2F(x,y) - (dx/dt)^2 + (dy/dt)^2$$

The three-dimensional set,

$$W = \{(x,y,dx/dt, dy/dt) \mid J = C\}$$

is called the Jacobi energy surface. It is a three-dimensional surface since one can solve for one variable in terms of the other three. The solutions for the differential equations for a specific value of C must lie on the surface $W(C) = \{J = C\}$.

As C varies, the Jacobi surfaces change their appearance. They can be viewed projected into position space. This yields regions in the (x,y) plane where SC can and can't move. The regions where SC can move are called Hill's regions¹. From the form of the Jacobi energy equation, they are defined by the relation, $2F(x,y) \geq C$. The regions where SC cannot move are called 'forbidden regions', and are dark grey in Figure 3. The Hill's regions change their geometry when C takes on the values C_k , $k = 1,2,3,4,5$, corresponding to the locations of the Lagrange points, L_k , where the velocity and acceleration of SC is 0, described in the next paragraph. More precisely, if we let $(x,y) = (a_k, b_k)$ be the locations of the L_k points, then $J(a_k, b_k, 0, 0) = C_k$. It turns out that $C_1 > C_2 > C_3 > 3 = C_4 = C_5$. For example, $C_1 = 3.2003449\dots$, $C_2 = 3.184164\dots$, $C_3 = 3.023159\dots$. As C decreases, SC can achieve higher velocities.

The Hill's regions are seen in Figure 3. In Figure 3a, $C > C_1$ and SC is trapped either about E or M. It doesn't have sufficient velocity to escape either body. When it decreases to $C = C_1$, the Hill's regions about M and about E meet exactly at the point L_1 between E and M. As C decreases slightly below C_1 we obtain 3b, where there is a small opening near L_1 where SC has sufficient velocity to pass between E and M. When $C_2 < C < C_1$, a small retrograde periodic orbit appears in the opening (or neck), called a Lyapunov orbit, we will discuss below. When $C = C_2$ the Hill's region squeezes to a point to the left of M which is L_2 , the exterior collinear point. As C decreases slightly below C_2 an opening appears about the L_2 location seen in 3c where the SC can escape the E,M system. Another retrograde Lyapunov periodic orbit appears in the opening. In this paper, we will be interested in the points L_1, L_2 and in particular L_2 . For $C > 3$, we have 3e and SC can move everywhere in the entire (x,y) -plane.

The boundary of the Hill's regions are curves where the velocity of SC is zero: $dx/dt = dy/dt = 0$. These are

called zero velocity curves. They are determined by setting the velocity equal to zero in the Jacobi energy, which yields, $2F(x,y) = C$. For example, in Figure 3b, a zero velocity is the peanut shaped curve going around both P_1 and P_2 .

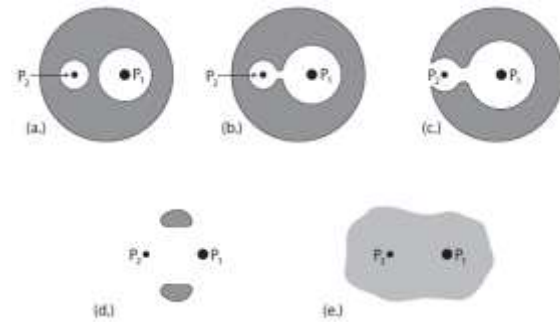


Figure 3 Variation of Hill's regions $W(C)$ as C varies. (in these figures, $M = P_2$ is placed to the left of $E = P_1$.)

The differential equations yield five points where both the acceleration and velocity are equal to zero. These are five locations in the (x,y) plane where SC remains fixed, called equilibrium points. Three of them lie on the x -axis and are called collinear points, L_1, L_2, L_3 , and two lie at the vertices of equilateral triangles, L_4, L_5 , called equilateral points. Their locations are shown in Figure 4. For example, in the case of L_1 and L_2 , with locations $(a_1, 0), (a_2, 0)$, respectively, $a_1 = .836914\dots$, $a_2 = 1.155682\dots$

To obtain real distances, these would be multiplied by the mean distance from E to M.

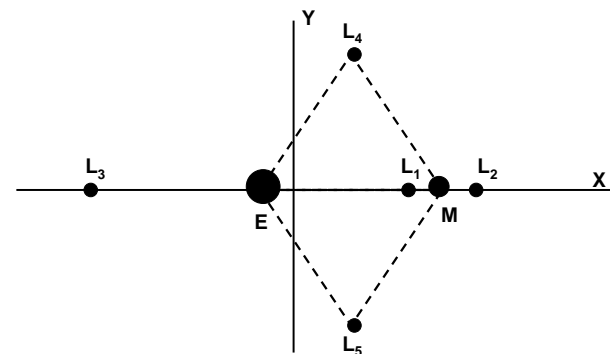


Figure 4 The Lagrange points

The collinear Lagrange points are unstable. This means that if SC were placed near any of these points, it would not remain there for long and move away from the location. This is because if one linearized the equations of motion at the collinear points, the solutions for the positions $x(t), y(t)$ near these points would contain exponential terms of the form e^{bt} , where $b > 0$, and e^{ct} , $c < 0$. These exponential terms define special

directions where SC moves towards a given collinear point, called stable directions, and special directions where SC moves away from the collinear point called unstable directions. Moreover, $x(t)$, $y(t)$ contain also multiplicative terms with $\sin At$, $\cos At$, $A > 0$. This causes SC to spiral as it is moving exponentially towards or away the Lagrange point. So, as time t increases, so do $x(t)$, $y(t)$. This type of unstable dynamics is due to the fact that the collinear points have a saddle point behavior.^{1,5}

Even though the dynamics near the collinear points is unstable, a family of periodic orbits exists about these locations parameterized by the Jacobi constant C . These periodic orbits are called Lyapunov orbits, or lissajous orbits. They are retrograde and in our current model, lie in the (x,y) -plane. These orbits are planar versions of halo orbits. Since the dynamics near the collinear Lagrange points is unstable, and saddle-like, this implies that the Lyapunov periodic orbits about L_k , $k=1,2,3$, labeled LO_k , are also unstable. The stable and unstable saddle-like behavior gives rise to special surfaces, in position-velocity space that the trajectories lie on called *invariant manifolds*. These manifolds look like tubes and emanate from the Lyapunov orbit. Two manifolds are called stable, and labeled $W^s(LO_k)$. Trajectories on them spiral towards LO_k . There are two unstable manifolds, $W^u(LO_k)$ where trajectories spiral away from LO_k . This is shown in Figure 5, where the Lyapunov orbit LO_1 is shown in the connecting neck between the Hill's regions about the Earth and Moon. The manifolds are projected onto the physical (x,y) -plane and exist in the Hill's regions.

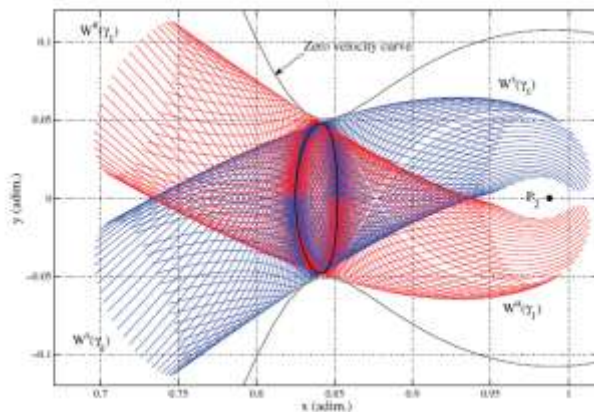


Figure 5 Lyapunov orbit γ_1 and associated manifolds

These manifolds move far from the Lyapunov orbit and can move near the Earth. This is utilized in this paper for LO_2 . If a trajectory moves on a stable manifold near the Earth, it can travel all the way to LO_2 and go

into orbit about it for no ΔV . That is, ballistic capture can be obtained about the Lyapunov orbit thus saving substantial propellant. This idea will guide our trajectory design later in the paper.

This is also the idea behind obtaining ballistic capture about the Moon. In this case the structure of the WSB where capture can take place is very complicated consisting of infinitely many intersections of the manifolds from the Lyapunov orbits forming a fractal like region, called a hyperbolic tangle⁵. This is crudely illustrated in the cartoon in Figure 6. This figure shows a trajectory, in red, moving to ballistic lunar capture at the WSB. This trajectory is assumed to come from an exterior WSB transfer mentioned earlier, that will be discussed later in this paper. The Jacobi energy C is slightly less than C_2 as in Figure 3c. The manifolds associated to L_1 , L_2 are seen to form a hyperbolic tangle about the Moon – which is too complicated to draw as it would have infinitely many intersections filling a large region around the Moon, forming a fractal set. The trajectory is seen to pass through the Lyapunov orbit about the L_2 location. This hyperbolic tangle is numerically demonstrated to represent the WSB¹⁵. More exactly, the Lyapunov orbits and global stable manifolds, $W^+_{L_1}$, $W^+_{L_2}$ comprise the WSB in this picture. This implies that ballistic capture transfers to $L_{1,2}$ are WSB transfers.

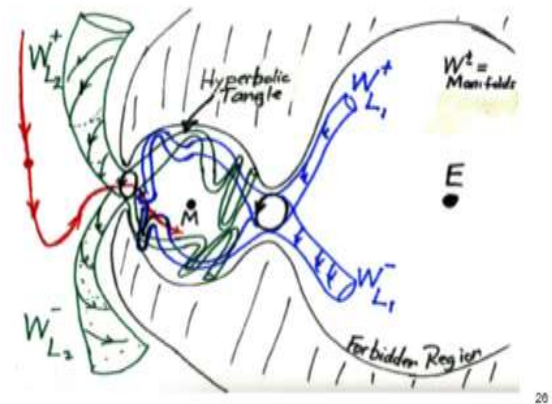


Figure 6 A trajectory from an exterior WSB transfer going to ballistic capture about the Moon

We conclude this section by mentioning that the WSB region was initially defined by a numerical algorithm in 1986¹¹. This algorithm is straight forward to model on the computer and basically represents the transition region between ‘stable’ and ‘unstable’ motion about this Moon^{15,16}. For a given starting point on a radial line, L , from the Moon, and propagating

trajectories along that line with fixed eccentricity, E , between 0 and 1, stable motion means that SC is able to perform one cycle about the Moon and return to L with negative Kepler energy wrt to the Moon, otherwise it is unstable. Unstable means that SC cannot return to L before going around the Earth, or returning to L with positive Kepler energy. This is illustrated in Figure 7. The WSB itself is a collection of all the critical distances r^* where the transition between stable and unstable motion occurs for each choice of E , and for each radial line making an angle θ with the x -axis, where the angle varies between 0 and 360 degrees.

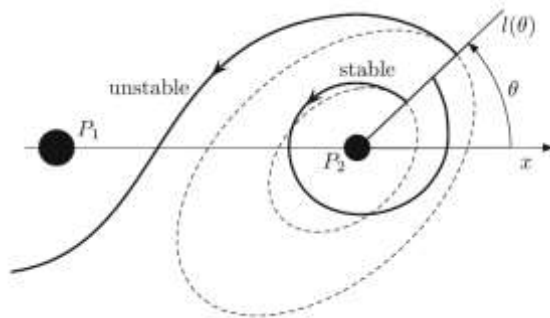


Figure 7 Stable and Unstable points after 1 cycle

This definition of the WSB was sufficient to find useful ballistic capture transfers, both interior and exterior; however, it was not sufficient to understand this region mathematically. In 2007, Garcia and Gomez published a paper¹⁴ that gave a definition that generalized the algorithm defining the WSB, where instead of determining the transition distance r^* after one cycle, they did this for n -cycles, $n=1,2,3,\dots$, forming a sequence of WSB's parameterized by n , say W_n . Moreover, along each line L , there was not just one value of r^* , but infinitely many, separated by intervals that alternate between stable and unstable motion. Taking the set of all r^* for $n=1,2,3,\dots$ yields the generalized WSB. A slice of the WSB about the Moon for $n=1$, $e=.3$ is shown in Figure 8. The plot shows the points comprising the stable motion. The WSB itself is the boundary of this region.

The WSB points are points where ballistic capture can occur. They have the property that the Kepler energy with respect to the Moon is negative. However, the motion is unstable, and chaotic. Fortunately for applications, a tiny ΔV of 10 m/s can stabilize the motion into a stable capture. To achieve a ballistic capture transfer from the Earth, it is the goal for trajectories to go to the WSB. Since the L_1, L_2 are also

in this region, then transfers to these points, and the Lyapunov orbits about them can also be obtained. The transfer for *Hiten*, as well as SMART1 and GRAIL, all went to this region about the Moon since this is necessary for ballistic capture.

It is remarked that the exterior WSB ballistic capture transfer, being a low energy transfer, saves energy by reducing the ΔV required to go to a low circular orbit about the Moon. If, for example, such an orbit had an altitude of 100 km, then the savings is about 25%. This can result in doubling the payload for the same launch vehicle, which was taken advantage of by the GRAIL mission, sending two spacecraft. On the other hand, if capture were desired with no maneuver at all, then the resulting capture osculating ellipse at 100 km periaapsis has an eccentricity of about .96. This property was used for the *Hiten* mission since the spacecraft had almost no propellant. The interior WSB transfer, also saves propellant by going to ballistic capture at the Moon about the L_1, L_2 points, but has a disadvantage to the exterior WSB transfer that it needs to start further from the Earth, at about 60,000 km, since it is required to reach the manifolds at that distance. The SMART1 mission did this by slowly spiraling out using SEP. As we'll show in the next section, if one starts from a parking orbit about the Earth of sufficiently large size, then these manifolds are easily reached in position as well as velocity.

The dynamics associated with the WSB region offers many exciting applications beyond ballistic capture that are beyond the scope of this paper. This includes ballistic ejection, resonance transitions, and applications to missions to Mars and other planets.

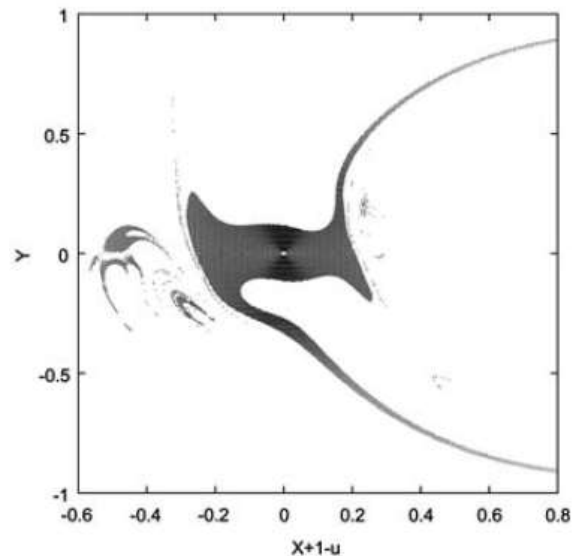


Figure 8 WSB stable region about the Moon for $n=1$, $e = .3$.¹⁴ (The Earth is one unit to the right). The boundary of this region is the WSB for $n=1$, W_1 . If this picture were magnified, there would be infinitely many gaps. As n increases, these regions become more sparse. All points on the WSB are points where ballistic capture can occur

IV. LOW-ENERGY TRANSFERS: ANALYSIS DEFINITION AND RESULTS

Analysis Definition and Results

This section describes results on the determination of new low energy transfers that go into orbit about the Earth-Moon L_2 point, starting from a highly elliptical Earth orbit that offer significant propellant savings to that of a Hohmann transfer. We will describe how to determine both interior and exterior low energy transfers that will ballistically transfer to Lyapunov(lissajous) orbits about L_2 . Two spacecraft systems will be examined. The first is a hybrid system consisting of both electric and chemical propulsion (SC1) and the other is purely chemical propulsion (SC2). The spacecraft are assumed to start in an elliptic parking orbit about the Earth, and go to a lissajous orbit about L_2 of particular dimensions. We use newly developed optimization software that is able to optimize the trajectories for both types of propulsion, and which also utilize the invariant manifolds, and the weak stability boundary. For SC1 we show that although the low energy transfers can achieve orbit about L_2 with significant margin, the Hohmann transfer does not have sufficient propellant. This underscores that the Hohmann transfer is neither suitable nor desired for transfer for orbit about L_2 for the spacecraft we are using and under our assumptions. We will also show that the exterior and interior transfers have comparable performance with respect to both propellant usage and time of flight. The interior transfer is shown to have better performance than the exterior transfer under certain situations. Although the exterior transfer gives better performance, in general, this may not be significant given the fact it travels 1.5 million km from the Earth whereas the interior transfer stays roughly within the Earth-Moon distance. Many cases have been determined for this study; however, we will only be showing a sample of these due to space. For the case of SC2, substantial propellant reduction is obtained with respect to the Hohmann transfer.

For our models we use the planar circular restricted three-body problem as described in the previous section, for the interior transfer, and a bi-circular planar restricted four-body problem for the exterior transfer. This four-body problem is obtained by adding the motion of the Sun in addition to the Moon, and assumes

it also lies in the EM-plane and the Sun moves in circular orbit with constant velocity¹. Although these are planar problems, the results are valid in three-dimensions and also with an ephemeris, with negligible modification. In fact, if we had started with three-dimensions and with a planetary ephemeris, better performance could likely be obtained. The numerical integrator is 10th order. The optimization method, developed by G. Mingotti, F. Topputo, and F. Bernelli-Zazzera¹⁷ uses an interesting dynamical approach which optimizes the trajectories by minimizing the total ΔV usage, for example, and following invariant manifolds, which are simultaneously computed. It is a direct transcription method. When low thrust is being used, the thrust magnitude as well as direction is varied over various time spans. The computation of the invariant manifolds makes this optimization well suited for low energy trajectories. Traditional optimization methods would be difficult, or not possible to use, due to the sensitive dynamics.

The results of our analysis are now described.

We consider two different spacecraft. The first, SC1, uses both chemical and electric thrusters. The second, SC2, uses only chemical thrusters. SC1 is more interesting since it uses two different types of engines. The high thrust is suitable for providing the impulsive ΔV to escape the Earth's gravity, and the low thrust engines are suitable for gradually maneuvering within the invariant manifolds.

The parameters for the two different spacecraft are:

SC1 (Hybrid)

Dry mass, $m_{dry} = 2669$ kg

Chemical propulsion

Propellant mass, $m_{p,ch} = 2100$ kg

Specific impulse, $I_{sp,ch} = 226$ s

Engine thrust, $T_{ch} = 40$ N

Number of engines, $N_{ch} = 4$

Low-thrust propulsion

Propellant mass, $m_{p,lt} = 434$ kg

Specific impulse, $I_{sp,lt} = 2000$ s

Engine thrust, $T_{lt} = 0.25$ N

Number of engines, $N_{lt} = 8$

SC2 (Chemical)

Dry mass, $m_{dry} = 5120$ kg

Propellant mass, $m_p = 6960$ kg

Specific impulse, $I_{sp} = 312$ s

Engine thrust, $T = 490$ N

Number of engines, $N = 4$

Statement of Problem and Assumptions

The spacecraft is assumed to be in a given parking orbit about the Earth it will depart from. It will then transfer to go into a lissajous orbit about L_2 .

Initial Parking Orbit

Perigee altitude, $h_p = 185$ km
 Apogee altitude, $h_a = 70000$ km

Desired L_2 lissajous orbit(L2O)

x-amplitude, $A_x = 25400$ km
 y-amplitude, $A_y = 60000$ km

Earth-Moon Parameters:

Earth-Moon mass ratio, $\mu = 0.0121506683$
 Earth-Moon distance, $l_{em} = 384405$ km
 Earth-Moon period, $T_{em} = 27.32$ days
 Gravitational acceleration at sea level, $g_0 = 9.806$ m/s²

Interior WSB Transfer

Statement of the problem

Case1 – SC1 – The spacecraft leaves the Earth parking orbit by applying a ΔV at the perigee of the parking orbit. The ΔV is achieved with chemical propulsion. After this impulse, the spacecraft uses low-thrust propulsion to target a point on the stable manifold associated to the final L_2 orbit, L2O. This transfer has to be computed by using the least propellant mass (sum of chemical and low-thrust propellant; i.e., the final mass in L_2 orbit has to be maximized).

Case 2 – SC2 – The spacecraft leaves the Earth parking orbit with an impulsive maneuver (DV1) and uses the chemical propulsion only to reach a point on the stable manifold associated to the L_2 orbit. Thus, another impulse, DV2, is needed to target the stable manifold. This leads to a two-impulse strategy. The goal is to minimize the sum $DV1+DV2$, so minimizing the chemical propellant spent (and, again, maximizing the mass in L_2 orbit, L2O).

Geometry of Problem

The geometry of the problem shows the relative distances involved and where the stable manifolds are that lead to L2O. This is plotted next,

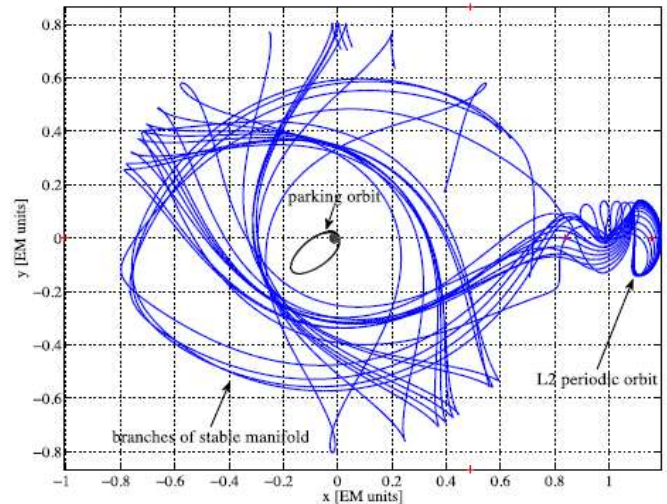


Figure 9 Geometry of the problem showing the initial parking orbit, the periodic Lyapunov orbit about L_2 , L2O, and trajectories on the stable manifold W_{L_2} that move to L2O

The initial parking orbit is clearly seen. Relative to the size of the stable manifold, the parking orbit is small. The figure shows not the stable manifold to L2O, but rather trajectories on it. The projection of the stable manifold onto the xy-plane is shown in Figure 5, which is the blue region to the left of L2O in the Hill’s region about the Earth. This manifold actually extends to go around the Earth, and some of the trajectories on it are shown in Figure 9. As is clearly seen, a maneuver at the periapsis of the parking orbit is needed to increase the apoapsis in order to reach the stable manifold.

SC1:

The methodology of the trajectory design for SC1 and optimization is as follows:

1. The first impulsive maneuver is used to raise the apoapsis of the parking orbit. After that, the low-thrust propulsion is used in the regions across the apoapsis to raise the periapsis. In this way the transfer orbit is “reshaped” to match the conditions of the stable manifold;
2. The L_2O stable manifold is reached when both position and velocity are matched;
3. The stable manifold is reached at the apoapsis. It has been demonstrated that this strategy is more convenient than inserting the spacecraft at the periapsis;
4. The small maneuver needed for the acquisition of L2O is not considered; this maneuver amounts to less than 1 m/s and can be ignored in this preliminary analysis.

Throughout these steps, the ΔV 's are minimized using the optimization procedure.

Several cases have been optimized and are presented. It is noted that this is a complicated optimization problem, and to obtain the best solution would require considerable time. To facilitate this, we have chosen reasonably good solutions. Further automating the software would enable more efficient searches.

To start the procedure an initial guess is required. This implies a guess on,

- a) The orientation of the parking orbit (i.e., argument of perigee),
- b) The magnitude of the impulsive DV (the direction is tangential to the perigee velocity),
- c) The duration of the low-thrust orbit,
- d) The magnitude of the low-thrust,
- e) The region where the low-thrust is effective,
- f) The duration and location of the stable manifold branch.

An example of what the initial guess is shown in Figure 10,

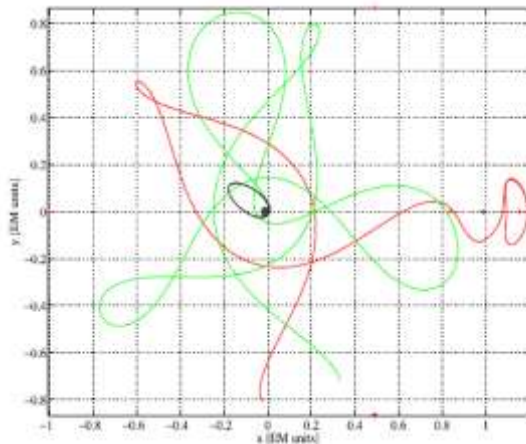


Figure 10 First guess for the optimizer for SC1. The parking orbit is shown. The green curve is the low thrust trajectory and the red curve is a trajectory on the stable manifold leading to L2O. The optimizer then iterates on this configuration.

The transfer optimization has the goal of minimizing the objective function while being constrained by the transfer parameters. It is performed with a direct transcription procedure. The dynamics is discretized over a uniform time grid and the equations of motion are integrated within each of the time intervals. The problem is formulated as a nonlinear programming problem and solved for a finite set of variables.¹⁷ In the case of hybrid transfers, the constraints are: 1. the final state of the low-thrust orbit has to be equal to the initial

state of the stable manifold branch; 2. the low-thrust profile must not exceed the maximum available thrust. The objective function is represented by the propellant mass (i.e., the final mass is maximized). The design variables are the low-thrust mesh points and the duration of the low-thrust phase.

We show a solution that has converged then give a table showing the numbers generated for several different cases. A converged solution for SC1 is shown in Figures 11a, 11b in different coordinate systems.

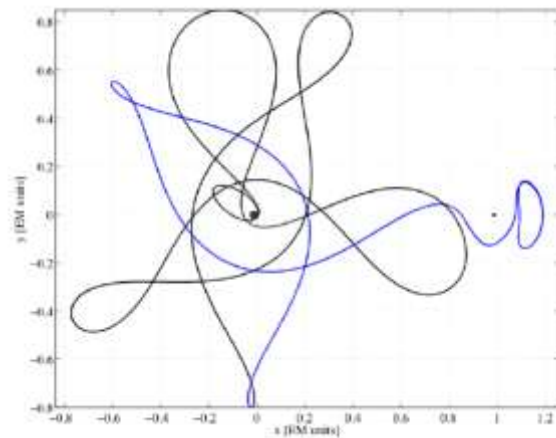


Figure 11a Converged solution for SC1 in a rotating coordinate system (Case 4). The black curve represents low thrust, and the blue is a stable manifold trajectory

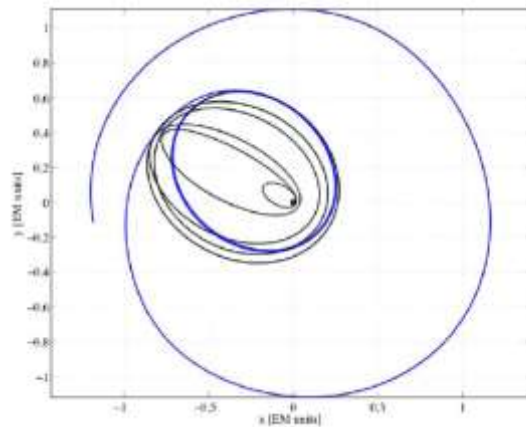


Figure 11b Converged solution in Figure 13a for Case 4, in an inertial coordinate system, Earth centered

In Figure 12a,b, a more complicated converged solution is shown (Case 2)

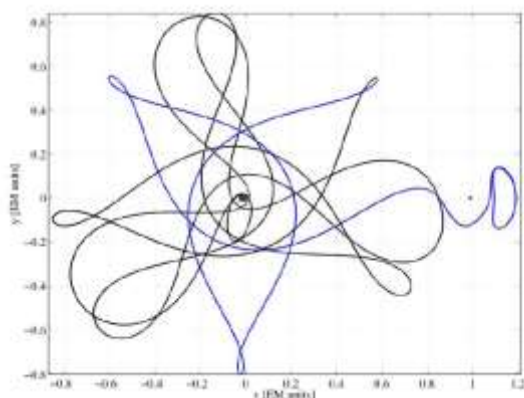


Figure 12a Converged solution for SC1 (Case 2) in a rotating coordinate system

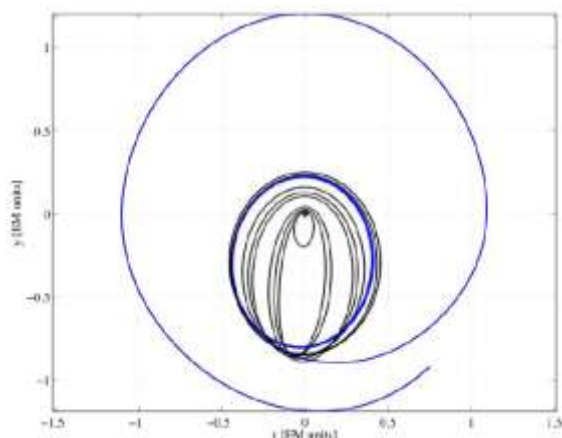


Figure 12b Solution in 12a (Case 2) in inertial coordinates

The numerical values of the converged parameter for the converged solutions are summarized in the Table 1 for Cases 1-4. The parameters are defined as follows:

- DT1, time of the low-thrust arc;
- DT2, time on the stable manifold;
- DT, total transfer time;
- DV, initial maneuver;
- mp,ch, chemical propellant consumed;
- mp,lt, low-thrust propellant consumed;
- mp, total propellant consumed;
- mf, final mass in L2 orbit.

Solution	DT1 (days)	DT2 (days)	DT (days)	DV (m/s)	mp,ch (kg)	mp,lt (kg)	mp (kg)	mf (kg)
#1	73.59	71.96	145.56	337.66	738.34	181.99	920.34	4282.65
#2	71.55	61.52	133.08	337.66	738.34	116.19	854.54	4348.45
#3	72.53	51.39	123.92	337.66	738.34	125.47	863.81	4339.18
#4	44.99	51.39	96.38	337.66	738.34	146.25	884.59	4318.40

Table 1 SC1 performance from converged solutions. (wet mass 6203 kg)

SC2

The procedure for this case is analogous to SC1, but has some differences.

The optimization of impulsive transfers is performed by minimizing the total $DV = DV1 + DV2$, where $DV1$ is the cost to leave the Earth parking orbit, and $DV2$ is the cost for injecting the spacecraft on the stable manifold. The constraint in this case is represented by the matching condition between the final state of the ballistic arc from the parking orbit to the location near the beginning of the stable manifold and the initial state of the stable manifold. The objective function is the total DV , whereas the optimization variables are: 1. the orientation of the parking orbit; 2. the magnitude of the initial impulse; 3. the duration of the bridge arc.

The initial guess consists of the following parameters,

- a) Orientation of the parking orbit,
- b) Magnitude of the first impulse (tangential direction),
- c) Duration of the ballistic arc (in green in Figure 13),
- d) Duration and locations of the stable manifold branch (in red in Figure 13).

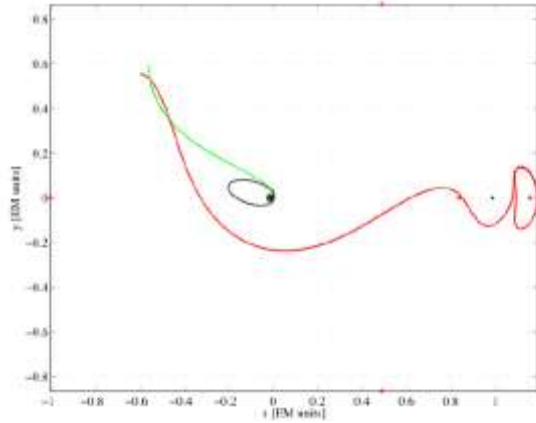


Figure 13 Initial guess for SC2. Green is a ballistic arc, and red is a trajectory on the stable manifold

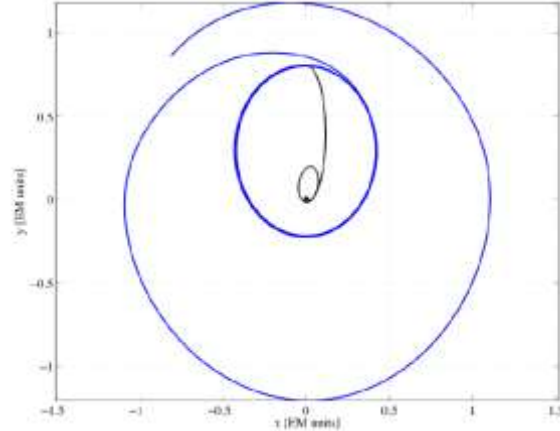


Figure 14b SC2 converged solution from Figure 14a in an inertial coordinate system, Earth centered.

A converged solution is shown in Figures 14a, 14b.

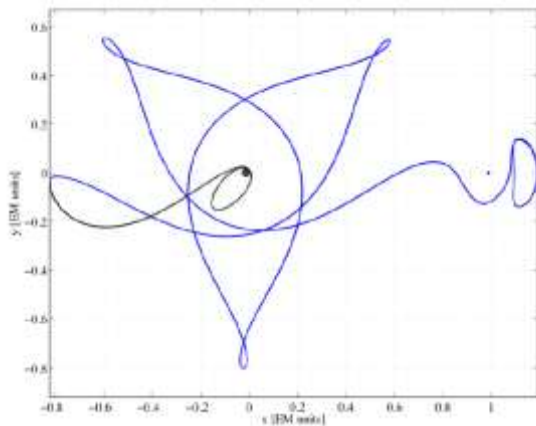


Figure 14a SC2 converged solution (Case 1)

Parameters for the converged cases for SC2:

- DT1, time of the bridge arc;
- DT2, time on the stable manifold;
- DT, total transfer time;
- DV1, cost for initial maneuver;
- DV2, cost for stable manifold injection;
- DV, total cost.

Solution	DV1 (m/s)	DV2 (m/s)	DV (m/s)	DT1 (days)	DT2 (days)	DT (days)
#1	330.30	542.25	872.56	3.66	71.96	75.62
#2	329.90	536.23	866.13	3.57	61.52	65.09
#3	329.44	516.50	845.95	3.56	51.39	54.95
#4	329.53	509.78	839.32	3.67	41.22	44.89

Table 2a Cost and transfer times for converged values for SC2

Solution	mp1 (kg)	mp2 (kg)	mp (kg)	mf (kg)
#1	1236.22	1761.22	2997.45	9082.54
#2	1234.80	1743.56	2978.37	9101.62
#3	1233.17	1684.93	2918.10	9161.89
#4	1233.49	1664.74	2898.23	9181.76

Table 2b Mass consumed for SC2 (wet mass 12080 kg).

It is remarked that SC1 could be targeted and optimized using only the chemical thrusters. In that case the performance is substantially worse than that shown in Table 1 using low thrust. *This is seen in Table 3 where the total propellant consumed is almost double to than*

for the hybrid system. This shows the efficiency of the hybrid system.

On the other hand, in Table 3, it is seen that

The total propellant consumed from SC1 only using the chemical thrusters is still substantially less than the Hohmann transfer considered next.

It is seen from Table 2b that SC2 saves approximately 1000 kg of propellant using the interior transfer, as compared to the Hohmann transfer, which is a very significant savings.

These results demonstrate the advantage in using low energy transfers.

Solution	mp1 (kg)	mp2 (kg)	mp (kg)	mf (kg)
#1	723.42	976.09	1699.51	3503.48
#2	722.61	966.68	1689.39	3513.69
#3	721.68	935.37	1657.01	3545.98
#4	721.86	924.47	1646.33	3556.66

Table 3 SC1 using only chemical thrusters

Hohmann Transfer

The propellant consumed for SC1, SC2 is now compared to a Hohmann transfer going to L2O from the same parking orbit. The Hohmann transfer uses only chemical thrusters.

In the Hohmann transfer the second impulse is used to inject the spacecraft directly in the L2 orbit. There is no use of the stable manifold. There is an infinite number of insertion points, and therefore there are infinite Hohmann transfers possible. We limit our analysis to only one of them, which is shown in Figure 15 (it is possible better performing Hohmann solutions exist, however it likely that they do not differ by too much).

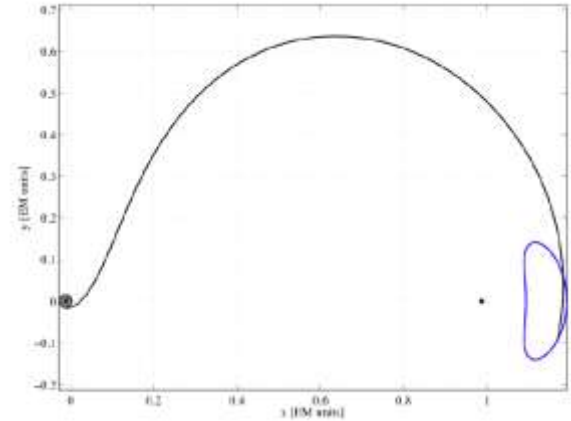


Figure 15 Hohmann transfer

The parameters of this Hohmann transfer are: $DV1 = 368.38$ m/s, $DV2 = 912.88$ m/s, $DV = 1281.88$ m/s, and $DT = 6.88$ days. This implies that the propellant consumption is 2284.44 kg for SC1 and 4133.22 kg for SC2.

We can obtain a significant conclusion from the propellant consumed.

The Hohmann transfer requires more propellant that is available from SC1 which is 2100 kg in chemical propellant. However, SC1 with the hybrid system uses less than 1000 kg, in total, as is seen in Table 1.

This underscores the efficiency of the hybrid system.

Exterior WSB Transfer

The previous analysis focused on the interior WSB transfer and it was seen that it had substantially better performance with respect to propellant consumption than the Hohmann transfer, where the best performance is from the hybrid system. In this section, we compute the exterior WSB transfer to L2O, using another stable manifold of LO2 and see how it compares to the interior transfer.

SC1

SC1 using a hybrid system - The spacecraft leaves the Earth parking orbit by applying a DV at the perigee of the parking orbit. The DV, achieved with chemical propulsion, places the spacecraft on an exterior low energy transfer, with maximum distance from the Earth of about three-to-five times the Earth-Moon distance. After this impulse, the spacecraft uses its own low-thrust propulsion system to target a point on the exterior stable manifold of L2O. This transfer is computed by

using the least propellant mass (sum of chemical and low-thrust propellant).

SC1 using only chemical propulsion – This transfer is similar to that of hybrid case except for the strategy used to insert the trajectory onto the exterior stable manifold of the L2O. In this case, another impulse, DV2, is needed to target the stable manifold. This leads to a two-impulse strategy. The aim is to minimize the sum DV1+DV2, so minimizing the chemical propellant spent.

The geometry of the problem and the location of the exterior stable manifold of L2O is seen in Figures 16a,b. Trajectories in the manifold are seen as the blue curves in (x,y)-coordinates, leading to L2O. The Hill's region is seen about the Earth, with an opening near L2O. The Jacobi constant of the associated(osculating) three-body problem must satisfy $C < C_2$. The capture region is magnified in Figure 16b.

The first impulse is given at the periapsis of the parking orbit. The impulsive ΔV at the periapsis allows us to increase the energy of the spacecraft with minimum DV.

The first impulse places the spacecraft on an exterior-like low energy transfer. This orbit has to reach a point of the exterior stable manifold in Figure 16a. As the transfer will be designed in the framework of the restricted four-body problem (a four-body dynamics is necessary for exterior WSB transfers), and the stable manifold is given, by definition, in the restricted three-body problem, it is desirable that the stable manifold is targeted as close as possible to the L_2 point, for the sake of preserving the accuracy of the solution.

In other words, the blue lines in Figure 16a are obtained in the Earth-Moon restricted three-body problem (the Sun perturbation is neglected), and the farther they extend from L_2 , the less accurate they are (because the Sun perturbation alters their dynamics). From this perspective, it is desirable that the insertion on the stable manifold occurs in the vicinity of L_2 , so that the piece of transfer defined on the stable manifold is preserved when the Sun perturbation is considered.

A very low ΔV is needed to target the stable manifold. From this cost, the amount of both the low-thrust and the chemical propellant is obtained by applying the rocket equation with proper parameters (Isp,lt and Isp,ch for the low-thrust and chemical, respectively).

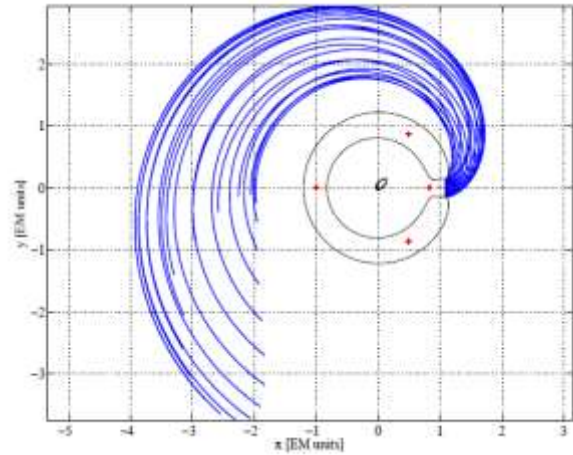


Figure 16a Geometry of the exterior stable manifold (blue) to L2O. Earth-Moon rotating frame.

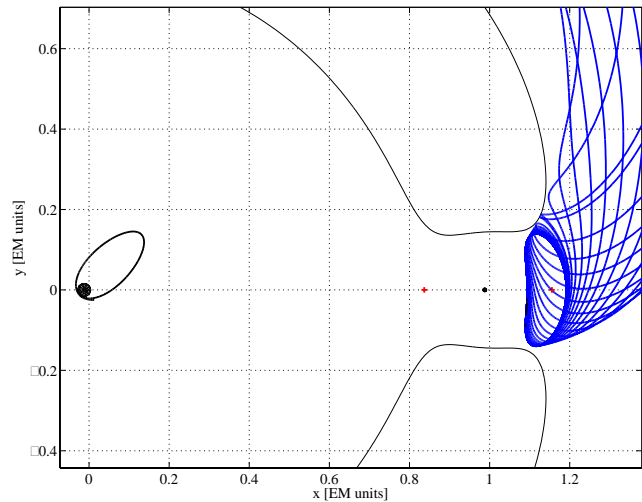


Figure 16b Magnification of Figure 16a

The problem is defined is as follows:

1. The model considered is the planar, bicircular restricted four-body problem with the Earth, the Moon, and the Sun as primaries,
2. The first impulse is used to raise the apoapsis of the parking orbit. After that, the low-thrust (or chemical) propulsion is used to adjust the orbit and target the exterior stable manifold,
3. The L2O orbit stable manifold is reached when both position and velocity are matched,
4. The small maneuver needed for the acquisition of the final L2O orbit is not considered; this

maneuver amounts to less than 1 m/s and can be ignored in this preliminary analysis.

A first guess solution is generated by specifying the following set of parameters.

- a) The orientation of the parking orbit (i.e., argument of perigee),
- b) The magnitude of the impulsive DV (the direction is tangential to the perigee velocity),
- c) The initial phase of the Sun,
- d) The duration of the exterior transfer,
- e) The duration and location of the stable manifold branch.

The optimization procedure is carried out in a similar way as with the previous problems. It turns out that the resulting nonlinear programming problem used to find the solution to this problem has (on average) about 100 variables. In this sense, this can be considered to be a 100 dimensional problem.

We compute five different exterior transfers. Four of them incorporate a lunar flyby when moving out to their apoapsis at about 1.5 million km, and one does not use a lunar flyby. The lunar flyby is used to decrease the propellant required to transfer to the apoapsis, and it also enables to match the beginning of the stable manifold to L2O more efficiently. (The *Hiten* mission used a lunar flyby) Two of them are shown in the following figures. Figures 17a,b show an exterior transfer which has a lunar flyby, and Figures 18a,b do not have a lunar flyby. The transfers without a lunar flyby are more generic, since critical timing is required to fly by the Moon. In this sense, the exterior without the lunar flyby is viewed as more typical. The results are summarized in Tables 4,5 for SO1 and in Table 6 for SO2. For all cases we define,

- DT, total transfer time;
- DTsm, time to the stable manifold;
- DV1, initial maneuver;
- DV2, stable manifold insertion maneuver;
- DV, total transfer cost
- mp1,ch, chemical propellant consumed in the initial maneuver (DV1).

For the hybrid case for SO1 in Table 4, we define,

- mp2,lt, low-thrust propellant consumed in the second maneuver (DV2);
- mp,lt total propellant consumed;
- mf,lt final mass in L2 orbit.

In Tables 5,6 for the fully chemical engines for SO1. SO2, we define,

- mp2,ch, chemical propellant consumed in the second maneuver (DV2);
- mp,ch total propellant consumed;
- mf,ch final mass in L2 orbit.

The time DTsm is given to indicate the time needed to reach the L2 neighborhood. Note that when the spacecraft reaches the stable manifold, the transfer is almost at the end of its trajectory, and it is necessary only to perform the final orbit injection. However, since the branch is defined on the stable manifold, it asymptotically flows towards L2O (and therefore takes long time to gradually converge to LO2 within given tolerances). The spacecraft may, in principles, begin operation before injecting into the final L2 orbit. In a first approximation we can think of DTsm as the Earth-L2O transfer time.

We will focus on the hybrid case since the performance of the chemical case is comparable, and is not quite as good.

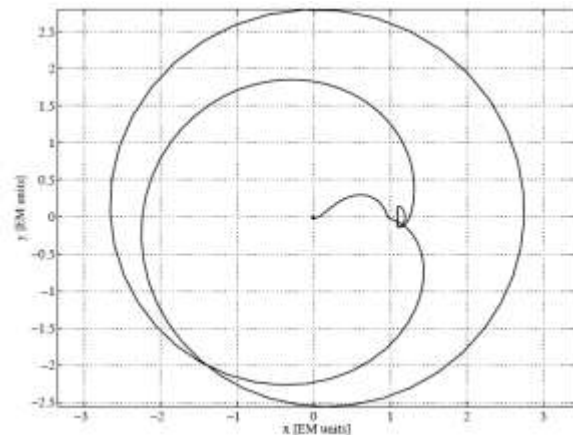


Figure 17a Exterior transfer with lunar gravity assist, Earth-Moon rotating frame (Solution 1)

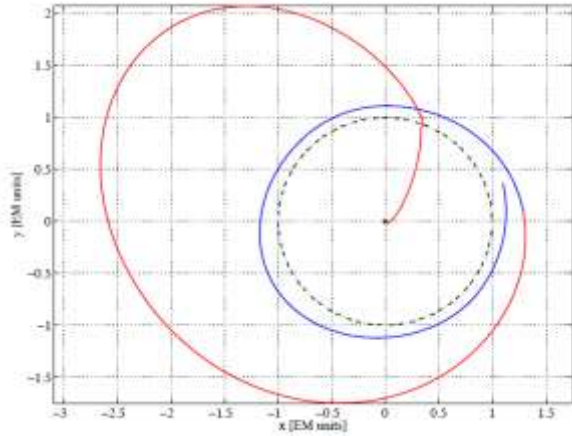


Figure 17b Exterior transfer in Figure 17a in an inertial frame (The red curve is the exterior transfer and the blue part lies on the stable manifold to L2O).

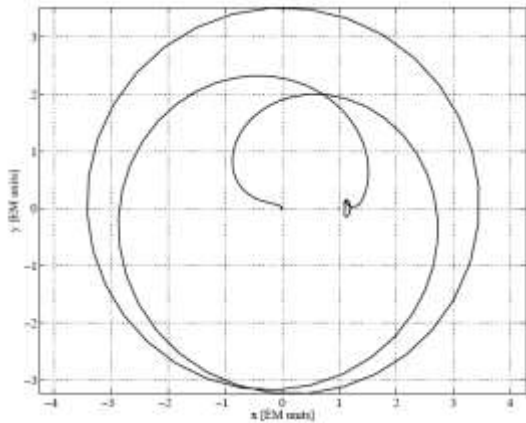


Figure 18a Exterior transfer without lunar gravity assist(Case 3)

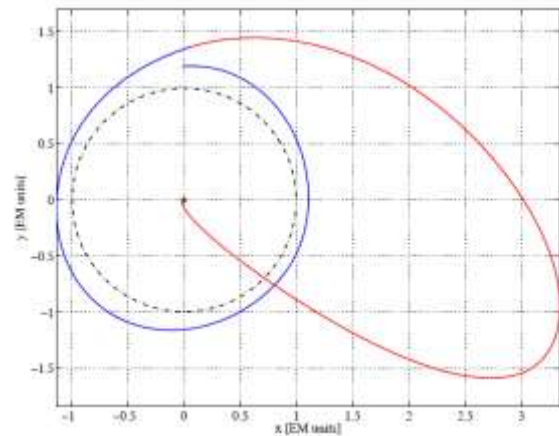


Figure 18b Exterior transfer – Case 3 in Figure 18a in an inertial coordinate system

Table 4 Exterior transfer performance for SC1, hybrid system(The best performing numbers are in bold)

Sc1	DT (days)	DTsm (days)	DV1 (m/s)	DV2 (m/s)	DV (m/s)	mp1,ch (kg)	mp2,ch (kg)	mp,ch (kg)	mf,ch (kg)
#1	104.75	80.83	350.00	24.15	374.15	763.23	48.34	811.58	4391.41
#2	99.18	73.09	349.77	63.32	413.10	762.78	125.62	888.41	4314.28
#3	103.46	77.81	413.58	203.97	617.55	889.34	180.92	1270.26	3932.73
#4	104.59	79.37	349.98	18.81	368.80	763.19	37.70	800.91	4402.09
#5	105.49	80.71	349.75	22.45	372.21	762.74	44.95	807.70	4395.29

Table 5 Exterior transfer for SC1 using only chemical engines

Performance of SC1

We consider the hybrid system. Case 3 is seen in Figures 18a,b. The performance of Case 3 is not as good as the other cases since it does not use a lunar gravity assist. In that sense, it is a more pure exterior transfer as discussed. Its total mass propellant used is 933.98 kg. If we compare this to the performance of SC1 for the interior transfer in Table 1, we see that the interior transfer out performs this exterior transfer by a significant margin. So, without the use of a lunar gravity assist, we can conclude that the interior transfer is better performing than the exterior transfer. In the remaining cases of the exterior transfer, Cases 1,2,4,5 perform better than the interior transfer since the lunar gravity assist reduces the ΔV required to transfer out to about 1.5 million km. It would be expected that a pure exterior transfer does not perform as well as an interior transfer since it needs to move much further from the Earth, as they both are captured at L2O ballistically. The better performance of the exterior transfer with the gravity assist is further enhanced since it can phase into the exterior stable manifold to L2O with less ΔV .

Sc1	DT (days)	DTsm (days)	DV1 (m/s)	DV2 (m/s)	DV (m/s)	mp1,ch (kg)	mp2,ch (kg)	mp,ch (kg)	mf,ch (kg)
#1	104.75	80.83	350.00	24.15	374.15	1305.83	84.74	1390.57	10689.42
#2	99.18	73.09	349.77	63.32	413.10	1305.03	220.73	1525.76	10554.23
#3	103.46	77.81	413.58	203.97	617.55	1527.41	680.61	2208.03	9871.97
#4	104.59	79.37	349.98	18.81	368.80	1305.76	66.06	1371.85	10708.17
#5	105.49	80.71	349.75	22.45	372.21	1304.97	787.88	1383.76	10696.24

Table 6 Exterior transfer performance for SC2

It is seen in Table 6 that SC2 saves a significant amount of propellant as compared to the Hohmann transfer, which is from 1900 to 2800 kg.

IV. CONCLUSION

The low energy trajectories perform significantly better than the Hohmann transfer with respect to propellant consumption. In fact, in the case of SC1, the Hohmann transfer does not even have sufficient propellant to transfer to L2O, whereas both the hybrid and chemical variants of SC1 have sufficient propellant. The hybrid system for SC1 out performs the chemical version of this system. The performance of the SC1 hybrid case is better than the pure exterior transfer for SC1, but not as good as the performance of the exterior transfer that does a lunar flyby. There is a large savings of propellant for SC2 using the interior and exterior transfers as compared to Hohmann

The low energy transfer optimization in both the interior and exterior cases, with hybrid systems, is complicated with many variables, on the order of 100 in the resulting nonlinear programming problem. Our analysis has only taken a look at a few cases and in the planar problem. It is seen to be necessary to more fully develop the optimization software so that the trajectory space can be explored more fully, and to do this in the case of three-dimensions which will give rise to a wider variety of solutions. The work we have presented clearly demonstrates that the low energy transfers to L2O, both interior and exterior, perform far better than the Hohmann with respect to propellant consumption.

The benefits derived by integrating high and low energy transfers range from system design and support to overall mission design mass savings and re-supply strategies. Different transfer design techniques can be explored by mission designers, testing various propulsive systems, maneuvers, rendezvous, and other in-space and surface operations. Understanding the availability of high and low energy trajectory transfer options opens up the possibility of exploring the human and logistics support mission design space and deriving solutions never before contemplated.

References

1. E. Belbruno, *Capture Dynamics and Chaotic Motions In Celestial Mechanics*. Princeton University Press, Princeton, NJ, 2004.
2. M. Raftery, J. Hoffman, ISS as a Base Camp for Beyond LEO Exploration, 62nd National Aeronautical Conference, Capetown, South Africa, October 2011
3. M. Brede, B.J.M. de Vries, *Networks that Optimize a Trade-Off Between Efficiency and Dynamical Resilience*, Published by Elsevier B.V., 2009
4. W. Hohmann, *Die Erreichbarkeit der Himmelskorper*, Oldenbourg, Munich, 1925. *Himmelsmechanik*, 1925
5. J. Guckenheimer, P. Holmes, *Nonlinear Oscillations, Dynamical Systems, and Bifurcations of Vector Fields*, Springer-Verlag, 1983.
6. E. Belbruno, Through the Fuzzy Boundary: A New Route to the Moon, *Planetary Report*, V7, May/June 1992.
7. E. Belbruno, J. Miller, Sun-Perturbed Earth-to-Moon Transfers with Ballistic Capture, *J. Guid, Control, and Dynamics*, V4, 770-775, 1993.
8. E. Belbruno, *Fly Me to the Moon*, Princeton University Press, Princeton, NJ, 2007.
9. H. Poincare, *Les Methodes Nouvelles de la mecanique Celeste*, Volumes 1,2,3, Gauthiers-Villars, Paris, 1892,93,99.
10. E. Belbruno, The Dynamical Mechanism of Ballistic Lunar Capture Transfers in the Four-Body Problem from the Perspective of Invariant Manifolds and Hill's Regions, CRM Research Report 270, Centre de Recerca Matematicam Institute d'Estudis Catalans, Barcelona, 1994.
11. E. Belbruno, Lunar Capture Orbits, A methods of Constructing Earth-Moon Trajectories and the Lunar GAS Mission, in *Proceedings of AIAA/DGGLR/JSASS Inter. Elec. Propl. Conf.*, no 87-1054, May 1987.
12. J. Schoenmaekers, , D. Horas,, J. Pulido, SMART-1: With Solar Electric Propulsion to the Moon, in *Proceedings of 16th Inter. Sym. On Space Flight Flight Dynamics*, Pasadena, CA, 2001.
13. W. Koon, M Lo, J. Marsden, S. Ross, Low Energy Transfer to the Moon, *Cel. Mech. Dyn. Astr.*, V 81, 63-73, 2001.
14. F. Garcia, G. Gomez, A Note on Weak Stability Boundaries, *Cel. Mech. Dyn. Astr.*, V97, 87-100, 2007.
15. E. Belbruno, M. Gidea, F. Topputo, Weak Stability Boundaries and Invariant Manifolds, *SIAM J. Appl. Dyn. Sys.*, V9, 1061-1089, Dec. 2010.
16. F. Topputo, E. Belbruno, Computation of the Weak Stability Boundaries: Sun-Jupite, *Cel. Mech. Dyn. Astr.* , V105, 3-17, 2009.
17. G. Mingotti, F. Topputo, and F. Bernelli-Zazzera, Optimal Low-Thrust Invariant Manifold Trajectories via Attainable Sets, *Journal of Guidance, Control, and Dynamics*, 34, 1644-1655, 2011